

A Domain Decomposition Method for the Exterior Helmholtz Problem

Romeo F. Susan-Resiga and Hafiz M. Atassi¹

*Department of Aerospace and Mechanical Engineering, University
of Notre Dame, Notre Dame, Indiana 46556*

E-mail: resiga@light.ame.nd.edu, atassi@carmen.ame.nd.edu

Received April 7, 1997; revised September 9, 1998

A new domain decomposition method is presented for the exterior Helmholtz problem. The nonlocal Dirichlet-to-Neumann (DtN) map is used as a nonreflecting condition on the outer computational boundary. The computational domain is divided into nonoverlapping subdomains with Sommerfeld-type conditions on the adjacent subdomain boundaries to ensure uniqueness. An iterative scheme is developed, where independent subdomain boundary-value problems are obtained by applying the DtN operator to values from the previous iteration. The independent problems are then discretized with finite elements and can be solved concurrently. Numerical results are presented for a two-dimensional model problem, and both the solution accuracy and convergence rate are investigated. © 1998 Academic Press

Key Words: Helmholtz equation; exterior problem; domain decomposition; non-reflecting boundary conditions; finite element method.

1. INTRODUCTION

In acoustics, the Helmholtz equation is the basic equation governing the propagation and scattering of time-harmonic sound. As a result, it has been extensively treated both analytically and numerically. However, as the field of applications extends to more complex problems and geometries, one needs to develop more accurate and powerful computational methods. Computational acoustics must resolve the waveform with minimum dispersion and dissipation. This requirement leads to a large number of grid points and, as a consequence, one ends up solving a very large system of equations. Numerical methods developed for solving such systems generally use iterative schemes. Because of the large memory requirements and to take advantage of parallel implementation, more recent iterative schemes are based on Schwarz domain decomposition wherein the computational domain is divided into several smaller subdomains which can be treated concurrently.

¹ Corresponding author.

There are, however, many fundamental issues associated with such methods. First, one needs to define the boundary conditions between adjacent subdomains so as to ensure uniqueness and convergence of the solution. Other issues are whether to consider underrelaxation and/or subdomain overlap as a way to accelerate the convergence of the scheme.

A domain decomposition numerical scheme will give a unique solution if the boundary-value problem associated with each subdomain has no eigen-solutions. Després [1] has shown that Sommerfeld-type boundary conditions between adjacent subdomains will lead to a unique solution of the Helmholtz equation in a given finite domain. Moreover, he has also shown that such a solution will converge to the exact solution of the boundary-value problem.

The present paper is concerned with developing a domain decomposition method (DDM) for an external scattering problem in an infinite domain. One important application for this class of problems can be found in aeroacoustics wherein a streaming motion interacts with a body and radiates sound in the far field. The governing equations for unsteady flows are the Navier–Stokes equations. However, because of the large memory and CPU time requirements in aeroacoustic computations, it is often possible [2, 3] to divide the flow domain into inner and outer regions with an overlapping area or simply separated by an artificial surface Γ as in Fig. 1. In the inner region surrounding the body, sound is generated as a result of the generally nonlinear interaction of the incoming flow with the body (the *nonuniform flow* region). In this sound-generating region the Navier–Stokes equations or, as often is the case, the Euler equations are used to model the flow. In the outer region, which may extend to infinity, sound propagates. If viscous dissipation is negligible in the outer region, the linearized Euler equations can then be used to model the propagating sound. Euler's equations linearized about a *mean uniform flow* can be reduced to a single Helmholtz equation for a function related to the pressure or to the unsteady potential, as shown in [2, 4].

In order to completely define the boundary-value problem for the inner (outer) region, a condition must be imposed along the outer (inner) boundary of this region in the overlapping case, or along the separating surface Γ . This condition also provides the coupling between the inner and outer fields, and an iteration mechanism for the two solutions. Moreover,

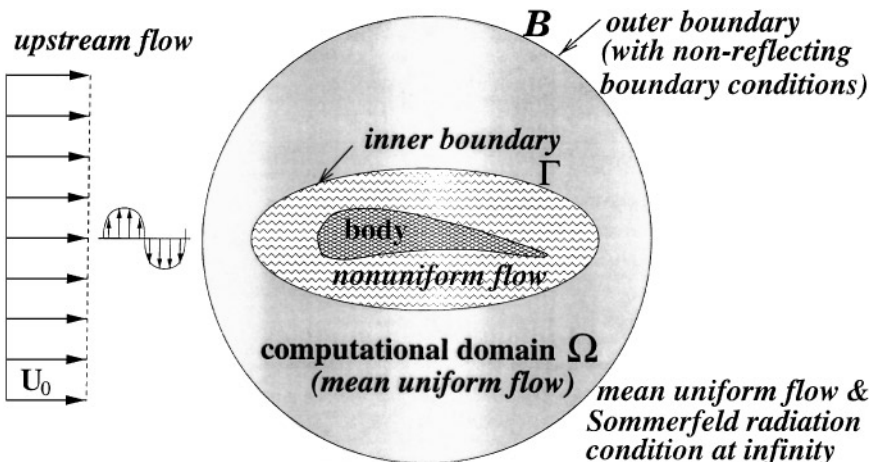


FIG. 1. Schematic of a body in nonuniform flow.

the causality principle leads to the usual Sommerfeld radiation condition for the outer boundary-value problem.

Since dispersion and dissipation errors are cumulative, numerical computations of unsteady flows may yield very accurate near- and mid-field solutions with inaccurate far-field results [4]. Therefore, in a general aeroacoustic/aerodynamic problem, one may first solve the inner problem by imposing, for example, a Sommerfeld radiation condition along its outer computational boundary [5]. The outer acoustic problem can then be solved with the Kirchhoff method, using the mid-field results of the inner problem [6, 7]. An iterative scheme may thus be developed by solving again the inner problem with conditions obtained from the solution of the outer problem, and so on. Details of an iterative scheme for nonoverlapping regions, consistent with Després [1] method, are given in Appendix A.

As already mentioned, the problem in the infinite domain exterior to Γ can be solved by using the Kirchhoff's method [3], with the benefit of a priori satisfaction of the radiation condition at infinity. However, this method introduces nonuniqueness at the characteristic wavenumbers of the corresponding homogeneous interior problem (which is not a property of solutions of the boundary-value problem in its original form) [8, p. 474]. Besides, if the Kirchhoff method is used with a free-space Green's function, one needs to specify along Γ both the values of the function and its normal derivative. These quantities are given by the inner solution. However, numerical differentiation introduces significant inaccuracies [4, 6]. The alternative would be to use a special Green's function which vanishes at the boundary Γ . This, however, requires the solution of an integral equation and will not be practical for a complex geometry [7].

An alternative to the boundary integral formulation for the outer region is a domain-based computation. For numerical implementation, one needs to transfer the radiation condition at infinity to an *outer computational boundary* \mathcal{B} surrounding the body at finite distance. At high frequency and high Mach number flows, the inner solution is very sensitive to spurious reflection from \mathcal{B} . It is therefore necessary to apply an exact nonreflecting boundary condition along \mathcal{B} . An exact analytical relation between the unknown function and its normal derivative, called Dirichlet-to-Neumann map (DtN), can be derived if \mathcal{B} is, for example, a circle (in two dimensions) or a sphere (in three dimensions) [9]. Note that this nonlocal DtN map involves the values of the unknown function over the whole artificial boundary \mathcal{B} .

In this paper we develop a domain decomposition numerical method to solve the Helmholtz equation in the outer *computational domain* Ω surrounded by the *inner* boundary Γ and *outer* boundary \mathcal{B} (Fig. 1). The approach uses the domain decomposition method with Sommerfeld boundary conditions along the adjacent surfaces between the subdomains, Dirichlet, Neumann, or Robin conditions along the *inner boundary* Γ , and the DtN map along the *outer boundary* \mathcal{B} . The finite element method is used to solve the boundary-value problem in each subdomain. There are several advantages introduced by the present method. *First*, instead of solving one large system of equations, one has to solve several independent smaller systems for each subdomain. This can be performed concurrently on parallel computers. Moreover, at every iteration only the right-hand vectors need updating while the subdomain matrices remain unchanged. *Second*, the nonlocal DtN map is applied to the known values on the outer boundary from the previous iteration and it does not add nonzero elements in the subdomain matrices.

In Section 2 the general boundary-value problem is formulated and the DtN map condition is introduced. In Section 3, the DDM is outlined and the boundary-value problem is formulated for every subdomain. Section 4 presents the new approach for solving the

exterior Helmholtz problem, which combines the DDM and the DtN map. In Section 5, numerical results using the present method are shown for a 2D model problem. Both the solution accuracy and the convergence rate are investigated. The conclusions are summarized in Section 6.

2. THE HELMHOLTZ PROBLEM IN AN EXTERIOR DOMAIN

Let Γ be a closed curve (in 2D) or a closed surface (in 3D) and \mathcal{D} , the infinite (unbounded) domain exterior to Γ . We consider the boundary value-problem for the Helmholtz equation,

$$\mathcal{L}\phi = 0 \quad \text{in } \mathcal{D}, \tag{1}$$

$$\frac{\partial\phi}{\partial\nu} + i\alpha\phi = g \quad \text{on } \Gamma, \tag{2}$$

$$\lim_{r \rightarrow \infty} r^{(d-1)/2} \left(\frac{\partial\phi}{\partial r} + ik\phi \right) = 0, \tag{3}$$

where $\mathcal{L} = \nabla^2 + k^2$ is the Helmholtz operator, k is the wavenumber, g is a given function on Γ , α is a real constant, $d = 2$ or 3 , the space dimension, $i = \sqrt{-1}$, the imaginary unit, and r is the distance measured from the origin taken near Γ ; $\partial\phi/\partial\nu$ denotes the outward normal derivative.

The condition at infinity (3) is the *Sommerfeld radiation condition*, which assures the uniqueness of the solution. For a finite computational domain Ω , one must introduce a *computational boundary* \mathcal{B} on which a new boundary condition which replaces (3) must be imposed. For this purpose it is convenient that \mathcal{B} be chosen to be a circle or a sphere of radius R , centered at the origin, for which the analytical solution in the exterior domain $\mathcal{D}' = \mathcal{D} - \Omega$, with Dirichlet conditions on \mathcal{B} and the Sommerfeld condition at infinity, is known. By differentiating this solution with respect to the radius r , one obtains the relationship between the function and its normal derivative,

$$\frac{\partial\phi}{\partial\nu} = \mathcal{M}\phi \quad \text{on } \mathcal{B},$$

where \mathcal{M} is the DtN operator [9].

For the two-dimensional Helmholtz equation with the boundary condition

$$\phi = \phi(R, \theta) \quad \text{on } \mathcal{B}, \tag{4}$$

and the radiation condition (3), the solution is

$$\phi(r, \theta) = \frac{1}{\pi} \sum_{n=0}^{\infty} \prime, \frac{H_n^{(2)}(kr)}{H_n^{(2)}(kR)} \int_0^{2\pi} \cos n(\theta - \theta') \phi(R, \theta') d\theta'. \tag{5}$$

The prime on \sum indicates that for $n = 0$ the coefficient is halved. $H_n^{(2)}$ is the Hankel function of the second kind.

The relation between the normal derivative of the function and its values on \mathcal{B} is obtained by formally differentiating (5) with respect to r and taking $r = R$:

$$\frac{\partial\phi}{\partial\nu}(R, \theta) = \mathcal{M}\phi(R, \theta) = \frac{k}{\pi} \sum_{n=0}^{\infty} \prime, \frac{H_n^{(2)\prime}(kR)}{H_n^{(2)}(kR)} \int_0^{2\pi} \cos n(\theta - \theta') \phi(R, \theta') d\theta' \quad \text{on } \mathcal{B}. \tag{6}$$

The boundary-value problem (1), (2), and (6) is equivalent to the variational problem: find $\phi \in H^1(\Omega)$ such that for all $w \in H^1(\Omega)$,

$$\int_{\Omega} (\nabla w \cdot \nabla \phi - k^2 w \phi) \, d\Omega + i\alpha \int_{\Gamma} w \phi \, d\Gamma - \int_{\mathcal{B}} w(\mathcal{M}\phi) \, d\mathcal{B} = \int_{\Gamma} w g \, d\Gamma, \quad (7)$$

where $H^1(\Omega)$ is the usual Sobolev space. To obtain a discrete form of this variational problem, we discretize Ω into a finite number of element subdomains, Ω^e , and within each element the function is approximated using the nodal values, ϕ_j^e , and the nodal basis functions, N_j^e :

$$\phi(\mathbf{x}) = \sum_j \phi_j^e N_j^e(\mathbf{x}).$$

The usual procedure of assembling the elements leads to a linear system of equations, with additional nonzero entries in the matrix from the nonlocal DtN map. If P and Q are two nodes on \mathcal{B} , then the corresponding DtN contribution is

$$\begin{aligned} \mu_{PQ} &= \int_{\mathcal{B}} N_P(\mathcal{M}N_Q) \, d\mathcal{B} \\ &= \frac{kR}{\pi} \sum_{n=0}^{\infty} \frac{H_n^{(2)'}(kR)}{H_n^{(2)}(kR)} \int_{\theta_P - \Delta\theta}^{\theta_P + \Delta\theta} \int_{\theta_Q - \Delta\theta}^{\theta_Q + \Delta\theta} N_P(R, \theta) N_Q(R, \theta') \cos n(\theta - \theta') \, d\theta \, d\theta'. \end{aligned} \quad (8)$$

For practical computations, the sum is truncated to a finite number of terms, N . Harari and Hughes [10] have shown that in order to guarantee the uniqueness of the solution, $N \geq kR$. An alternative approach has been proposed by Grote and Keller [11], which keeps the exact DtN for the first N modes (where N can be smaller than kR) while using the Sommerfeld condition for the higher order modes. This ensures the uniqueness of the solution in the computational domain and, in general, improves upon the accuracy.

In the present paper we are using quasilinear quadrilateral elements. If we assume constant angular spacing, $\Delta\theta$, between the nodes along \mathcal{B} , then the double integral in (8) can be expressed analytically [12],

$$\mu_{PQ} = \frac{kR}{\pi} \sum_{n=0}^{\infty} \frac{H_n^{(2)'}(kR)}{H_n^{(2)}(kR)} \frac{4(1 - \cos n\Delta\theta)^2}{\Delta\theta^2 n^4} \cos n(\theta_P - \theta_Q). \quad (9)$$

In the above expression, the term for $n = 0$ is obtained by taking the limit for $n \rightarrow 0$ and is equal to $-[H_1^{(2)}(kR)/H_0^{(2)}(kR)](\Delta\theta)^2$. Note that the series in (9) is convergent because for large n we have $H_n^{(2)'}(kR)/H_n^{(2)}(kR) \sim -n/(kR)$. Therefore we can satisfy the condition $N \geq kR$ with minimal computational effort.

The computational aspects of the nonlocal DtN in conjunction with the finite element method (FEM) are discussed in [9, 13]. The major inconvenience due to the additional nonzero elements introduced by the DtN operator in the global matrix has been addressed by Malhotra and Pinsky [14]. By recognizing that an iterative solver involves a matrix–vector product, they proposed that this product be evaluated at the element level without the explicit assembly of any global matrices. As a result, by eliminating the full matrix

storage, this methodology reduces both the memory requirements and the computational cost in comparison with the implementation proposed by Keller and Givoli [9].

The scheme we propose in this paper uses a different approach to overcome the problems associated with the nonlocality of the DtN map. Instead of solving a global system of equations, we are dividing the computational domain into several nonoverlapping subdomains and then solving independently smaller systems of equations. For each subdomain only Sommerfeld-type boundary conditions are imposed (i.e., the quantity $\partial\phi/\partial\nu + ik\phi$ is prescribed), except eventually for the portion of Γ for the subdomains adjacent to the inner boundary. An iterative technique is employed to update the subdomain boundary conditions so that the correct global solution is recovered. The DtN operator *acts* only on the values from the *previous* iteration (known) to find the boundary conditions for the current iteration and it does *not* add additional nonzero elements in the subdomain matrices. Thus for a structured grid one can efficiently use a band matrix storage for each subdomain.

3. DESPRÉS DOMAIN DECOMPOSITION METHOD FOR THE HELMHOLTZ EQUATION

Després [1] proposed an iterative nonoverlapping DDM for the Helmholtz problem,

$$\mathcal{L}\phi = f \quad \text{in } \Omega, \tag{10}$$

$$\frac{\partial\phi}{\partial\nu} + ik\phi = g \quad \text{on } \partial\Omega, \tag{11}$$

where Ω is a bounded open set in \mathbf{R}^d and $\partial\Omega$ is its boundary.

The main idea was to choose Sommerfeld-type transmission condition between subdomains so that there are no real eigenvalues for the inner homogeneous problem, and the DDM is well posed. This leads to the following iterative scheme,

$$\mathcal{L}\phi_i^{m+1} = f \quad \text{in } \Omega_i, \tag{12}$$

$$(\partial_{\nu_i} + ik)\phi_i^{m+1} = (-\partial_{\nu_j} + ik)\phi_j^m \quad \text{on } \Sigma_{i,j}, \tag{13}$$

$$(\partial_{\nu_i} + ik)\phi_i^{m+1} = g \quad \text{on } \Sigma_i, \tag{14}$$

where Ω_i is a finite sequence of nonoverlapping open sets embedded in Ω such that $\bar{\Omega} = \cup \bar{\Omega}_i$, $\Sigma_{i,j} = \bar{\Omega}_i \cap \bar{\Omega}_j$ for contiguous Ω_i and Ω_j , $\Sigma_i = \bar{\Omega}_i \cap \partial\Omega$ and m is the iteration index.

The convergence proof was done by considering the following homogeneous problem for the error $e^m = \phi - \phi^m$,

$$\mathcal{L}e_i^{m+1} = 0 \quad \text{in } \Omega_i, \tag{15}$$

$$(\partial_{\nu_i} + ik)e_i^{m+1} = (-\partial_{\nu_j} + ik)e_j^m \quad \text{on } \Sigma_{i,j}, \tag{16}$$

$$(\partial_{\nu_i} + ik)_i^{m+1} = 0 \quad \text{on } \Sigma_i. \tag{17}$$

If we introduce the boundary error energy calculated along the subdomain boundaries,

$$E^m = \sum_i \int_{\partial\Omega_i} \left(|\partial_{\nu_i} e_i^m|^2 + k^2 |e_i^m|^2 \right),$$

then it is possible to establish

$$E^{m+1} = E^m - 4k^2 \int_{\partial\Omega} |e^m|^2. \tag{18}$$

Since E is positive, $E \rightarrow 0$ as the iterations evolve and, consequently, $e_i^m \rightarrow 0$.

4. THE DOMAIN DECOMPOSITION METHOD WITH DIRICHLET-TO-NEUMANN MAP

Using the concept of Sommerfeld-type transmission conditions we have constructed the following DDM nonoverlapping scheme for the boundary-value problem (1), (2), and (6),

$$\mathcal{L}\phi_i^{m+1} = 0 \quad \text{in } \Omega_i, \tag{19}$$

$$\frac{\partial\phi_i^{m+1}}{\partial\nu_i} + i\alpha\phi_i^{m+1} = g \quad \text{on } \Gamma_i, \tag{20}$$

$$(\partial_{\nu_i} + ik)\phi_i^{m+1} = (-\partial_{\nu_j} + ik)\phi_j^m \quad \text{on } \Sigma_{i,j}, \tag{21}$$

$$(\partial_{\nu_i} + ik)\phi_i^{m+1} = (\mathcal{M}\phi^m)_i + ik\phi_i^m \quad \text{on } \mathcal{B}_i, \tag{22}$$

where $\Gamma_i = \Gamma \cap \partial\Omega_i$, $\mathcal{B}_i = \mathcal{B} \cap \partial\Omega_i$, and \mathcal{M} denotes the DtN operator. Note that we have replaced in the right-hand side of (22) the normal derivative $\partial_{\nu}\phi^m$ by its exact expression $\mathcal{M}\phi^m$ which satisfies the condition at infinity (3).

For the first iteration, the right-hand side terms in (21) and (22) are taken to be zero.

In order to investigate the convergence of the new iterative scheme, one wants to obtain an energy-type equation similar to (18), starting with the following homogeneous problem for the error $e^m = \phi - \phi^m$,

$$\mathcal{L}e^{m+1} = 0 \quad \text{in } \Omega_i, \tag{23}$$

$$\frac{\partial e_i^{m+1}}{\partial\nu_i} + i\alpha e_i^{m+1} = 0 \quad \text{on } \Gamma_i, \tag{24}$$

$$(\partial_{\nu_i} + ik)e_i^{m+1} = (-\partial_{\nu_j} + ik)e_j^m \quad \text{on } \Sigma_{i,j}, \tag{25}$$

$$(\partial_{\nu_i} + ik)e_i^{m+1} = (\mathcal{M}e^m)_i + ik e_i^m \quad \text{on } \mathcal{B}_i. \tag{26}$$

If we define the boundary error energy as

$$E = \sum_i \int_{\partial\Omega_i} (|\partial_{\nu_i} e_i|^2 + k^2 |e_i|^2) - (\alpha - k)^2 \int_{\Gamma} |e|^2 \tag{27}$$

then it can be shown (see Appendix B) that

$$\begin{aligned} E^{m+1} - E^m &= \int_{\mathcal{B}} (|\mathcal{M}e^m + ik e^m|^2 - |-\partial_{\nu} e^m + ik e^m|^2) \\ &= \int_{\mathcal{B}} \{ |\mathcal{M}e^m|^2 - |\partial_{\nu} e^m|^2 + 2k [\Im(\overline{e^m} \mathcal{M}e^m) + \Im(\overline{e^m} \partial_{\nu} e^m)] \}, \end{aligned} \tag{28}$$

where $\overline{e^m}$ is the complex conjugate of e^m and \Im denotes the imaginary part. Note that if we take $\mathcal{M}e^m = \partial_\nu e_m = -ike^m$, which corresponds to Després iteration scheme, Eq. (28) reduces to (18).

The two-dimensional DtN map can be rewritten as

$$(\mathcal{M}\phi^m)(R, \theta) = \frac{k}{\pi} \sum_{n=0}^{\infty} c_n^{(2)} \int_0^{2\pi} \cos n(\theta - \theta') \phi^m(R, \theta') d\theta', \quad (29)$$

with

$$c_n^{(2)} = \begin{cases} \frac{-H_1^{(2)}(kR)}{2H_0^{(2)}(kR)} & \text{for } n = 0, \\ \frac{H_{n-1}^{(2)}(kR) - H_{n+1}^{(2)}(kR)}{2H_n^{(2)}(kR)} & \text{for } n \geq 1, \end{cases}$$

where $\Im c_n^{(2)} < 0$ and is bounded [10]. If we assume only that $\mathcal{M}e^m \approx \partial_\nu e^m$, and substitute this in (28), we obtain

$$E^{m+1} - E^m = 4k \int_B \Im(\overline{e^m} \mathcal{M}e^m) = 4k^2 \left[\frac{R}{\pi} \sum_{n=0}^{\infty} (\Im c_n^{(2)}) C_n^m \right] < 0, \quad (30)$$

where

$$C_n^m = \left| \int_0^{2\pi} \cos(n\theta) e^m(R, \theta) d\theta \right|^2 + \left| \int_0^{2\pi} \sin(n\theta) e^m(R, \theta) d\theta \right|^2 > 0.$$

As a result, it can be seen that the energy defined by (27) decreases at each iteration as m increases.

5. NUMERICAL RESULTS

In order to assess our computational approach, we consider a model problem with a known analytical solution. Figure 2 shows this model problem, which consists of a source

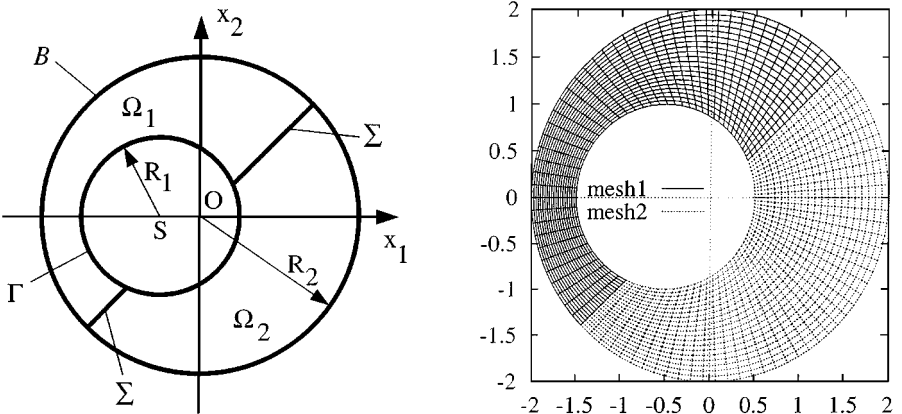


FIG. 2. The computational domain and the finite element mesh.

located at a point S in an unbounded domain and radiating sound. The potential associated with such a sound source can be written as

$$\phi = H_0^{(2)}(kr_s),$$

where r_s is the distance to the source S .

The corresponding computational problem is constructed as follows. A circle centered on S and of radius R_1 is taken to be the inner boundary Γ , along which a Neumann condition,

$$\frac{\partial \phi}{\partial \nu} = kH_1^{(2)}(kR_1),$$

is applied. The outer boundary \mathcal{B} is a circle centered at the origin O with radius R_2 . The computation domain between the nonconcentric circles Γ and \mathcal{B} is divided into two nonoverlapping subdomains Ω_1 and Ω_2 by a boundary Σ consisting of the intercept between Γ and \mathcal{B} of a line passing by the origin.

The wavenumber was taken $k = \pi$. Four noded quadrilateral elements are used to discretize the subdomain boundary value problems. Figure 2 also shows the finite element mesh for each subdomain.

For the first iteration, the following Sommerfeld-like boundary conditions were assumed on the subdomain boundaries except Γ ,

$$(\partial_{\nu_i} + ik)\phi_i^0 = 0 \quad \text{on } \mathcal{B} \text{ and } \Sigma.$$

The next iterations are performed using one of two kinds of boundary conditions on \mathcal{B} :

(a) Sommerfeld-like,

$$(\partial_{\nu_i} + ik)\phi_i^{m+1} = 0 \quad \text{on } \mathcal{B}_i.$$

(b) DtN map,

$$(\partial_{\nu_i} + ik)\phi_i^{m+1} = (\mathcal{M}\phi^m)_i + ik\phi_i^m \quad \text{on } \mathcal{B}_i.$$

At every iteration, for each subdomain Ω_i we have to solve a system of linear equations of the form

$$[A_i]\{\phi_i^{m+1}\} = \{b_i^{m+1}\}.$$

Note that only the right-hand vector is modified from one iteration to another; the matrix $[A_i]$ remains unchanged. This is an *important* advantage because the system matrix needs to be constructed only once. Moreover, after computing the LU factorization for the subdomain matrices, solving a sequence of linear systems for different right-hand vectors can be performed at a reduced computational cost.

For the numerical implementation of the iteration equation (21) on the subdomain interfaces we take advantage of the finite element formulation. If P is a node on the interface Σ_{ij} , then the corresponding entries in the right-hand vector at the iteration $m + 1$ can be computed as

$$\begin{aligned} \{b_i^{m+1}\}_P &= -[\bar{A}_j]_P \{\phi_j^m\}, \\ \{b_j^{m+1}\}_P &= -[\bar{A}_i]_P \{\phi_i^m\}, \end{aligned}$$

where $[\bar{A}_j]_P$ and $[\bar{A}_i]_P$ are the complex conjugates of the rows corresponding to the node P in $[A_j]$ and $[A_i]$, respectively. When P is at the intersection between the subdomain interfaces Σ and the inner or outer boundaries, the above equations are modified to accommodate the boundary conditions on Γ and \mathcal{B} , respectively.

A quantity which can be used to evaluate the convergence of the iterative scheme is the norm

$$\beta^{m+1} = \sum_i \|[A_i]\{\phi_i^{m+1}\} - \{b_i^m\}\|_2, \tag{31}$$

which in our case quantifies in some sense the change in the right-hand vector from one iteration to another. The iterations can be terminated when β becomes smaller than a given value.

For this particular model problem, we can also estimate the accuracy of the numerical solution in comparison to the analytical one. For each node n one can define the relative error,

$$\varepsilon_n^m = \frac{|(\phi_n^m)_{\text{numeric}} - (\phi_n)_{\text{analytic}}|}{|(\phi_n)_{\text{analytic}}|}. \tag{32}$$

This is a local indicator for the solution accuracy. A global accuracy parameter can be defined as the average relative error

$$\overline{\varepsilon^m} = \frac{\sum_n \varepsilon_n^m}{\text{number of nodes}}. \tag{33}$$

Of course, the norm β^m can always be defined, while ε_n^m requires knowledge of the analytical solution. For the present model problem, as will be shown below, the two parameters have a similar behavior as the iterations evolve.

Figure 3 shows the relative error, ($\text{err}[\%] = 100 \varepsilon_n$), distribution for the converged solution. First, it can be seen that the Sommerfeld condition on \mathcal{B} leads to spurious reflections with local relative errors up to 15%. The DtN map leads to the correct solution with 0.2% average error. Second, the iterative scheme practically eliminates the discontinuities at the subdomain interfaces.

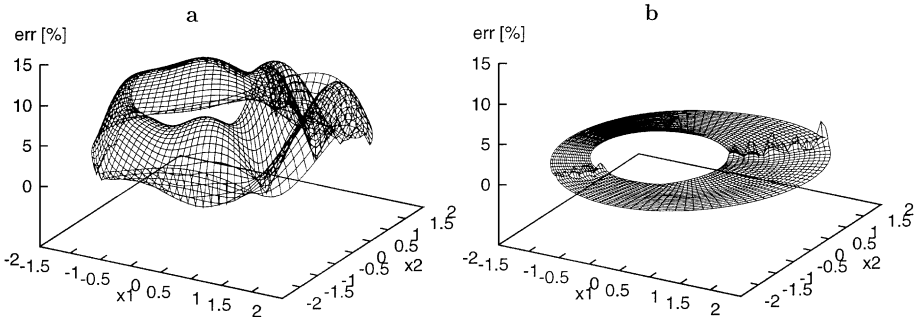


FIG. 3. The error distribution for (a) Sommerfeld-like boundary condition and (b) Dirichlet-to-Neumann map on \mathcal{B} .

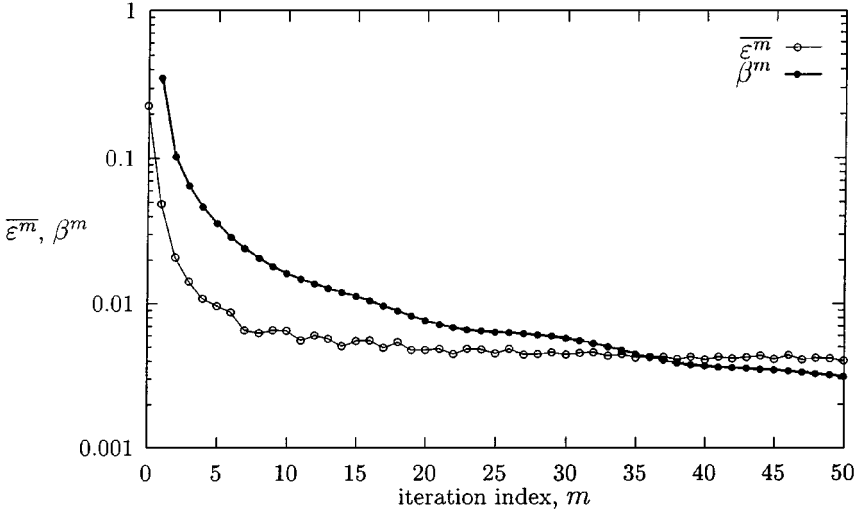


FIG. 4. The convergence history with DtN map on the outer boundary.

Figure 4 presents the convergence history for both the norm β and the average relative error $\bar{\epsilon}$. Note that the two parameters have similar behavior, although only β can be evaluated for a general problem. Practically, an acceptable solution is obtained after 10 iterations.

It should also be mentioned that the convergence rate can be improved by using underrelaxed iterations for the nonoverlapping DDM [15], or by using an overlap [16]. However, for the present paper, we limit our analysis to the application of the domain decomposition algorithm in conjunction with the DtN map.

6. CONCLUSIONS

This paper presents a domain decomposition method for solving the Helmholtz equation in the infinite domain exterior to an arbitrary boundary Γ . The finite computational domain is obtained by surrounding Γ with an outer boundary \mathcal{B} . By choosing \mathcal{B} to be a circle (2D) or a sphere (3D) and using the DtN map, the boundary conditions can be specified analytically.

Because the computational domain may be too large, it is divided into several subdomains in which the boundary-value problem can be solved independently. The global solution is obtained by iteration.

This new method has the following advantages:

- Although the DtN operator \mathcal{M} is nonlocal, the present method applies \mathcal{M} on the values of the unknown function from the previous iteration and thus it does *not* introduce additional non-zero elements in the subdomain matrix.
- The method is particularly suitable for parallel computing since at each iteration one solves several *independent* boundary-value problems.
- The matrix obtained by assembling the finite element matrices does not change from one iteration to another; only the right-hand vector must be updated at each iteration, therefore reducing the computational cost.

In conclusion, the use of DDM has removed the nonlocality drawback of DtN, leading, at the same time, to a parallel algorithm.

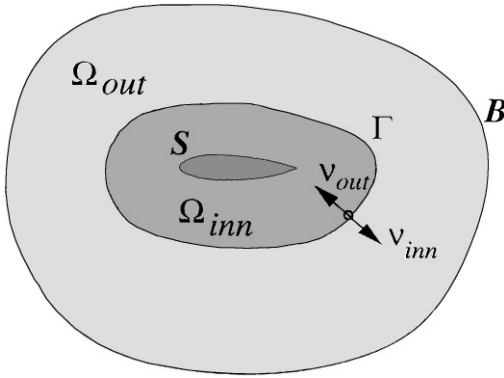


FIG. 5. Schematic for the inner and outer computational regions.

APPENDIX A: ITERATIVE SCHEME FOR NONOVERLAPPING INNER AND OUTER REGIONS

Consider a computational domain Ω surrounding the body S and surrounded at large distance by a surface \mathcal{B} . We divide Ω into an inner region, Ω_{inn} , and an outer region, Ω_{out} , by a surface Γ , as shown in Fig. 5.

Let ν_{inn} and ν_{out} be the unit normals to Γ outward of Ω_{inn} and Ω_{out} , respectively ($\nu_{inn} = -\nu_{out}$). The arbitrary surface Γ is located at a distance from S such that the unsteady flow in Ω_{out} is outside the strong interaction zone surrounding the body, and the flow is governed by the Euler equations linearized about a uniform mean flow. It is then possible to assume that in the neighborhood of Γ this linearization is valid and that on either side of Γ these equations can be reduced to a single Helmholtz equation for functions ϕ_{inn} and ϕ_{out} related to the unsteady pressure. Thus, we have

$$(\nabla^2 + k^2)\phi_{inn} = 0, \tag{34}$$

$$(\nabla^2 + k^2)\phi_{out} = 0, \tag{35}$$

$$\mathcal{R}(\phi_{out}) = 0 \quad \text{along } \mathcal{B}, \tag{36}$$

where we have assumed that ϕ_{out} satisfies a radiation condition (36) along \mathcal{B} . The flow in Ω_{inn} is, in general, governed by a system of nonlinear equations (Navier–Stokes or Euler) with specified conditions along S .

In order to complete the two boundary-value problems, we propose the following iterative scheme:

1. The inner boundary-value problem is first solved with the condition

$$\frac{\partial \phi_{inn}^{(0)}}{\partial \nu_{inn}} + ik\phi_{inn}^{(0)} = 0 \quad \text{along } \Gamma. \tag{37}$$

2. The outer boundary-value problem, (35) and (36), is solved with the condition

$$\frac{\partial \phi_{out}^{(0)}}{\partial \nu_{out}} + ik\phi_{out}^{(0)} = -\frac{\partial \phi_{inn}^{(0)}}{\partial \nu_{inn}} + ik\phi_{inn}^{(0)} = 2ik\phi_{inn}^{(0)} \quad \text{along } \Gamma. \tag{38}$$

3. The inner problem is then solved with

$$\frac{\partial \phi_{\text{inn}}^{(1)}}{\partial \nu_{\text{inn}}} + ik\phi_{\text{inn}}^{(1)} = -\frac{\partial \phi_{\text{out}}^{(0)}}{\partial \nu_{\text{out}}} + ik\phi_{\text{out}}^{(0)} = 2ik(\phi_{\text{out}}^{(0)} - \phi_{\text{inn}}^{(0)}) \quad \text{along } \Gamma, \quad (39)$$

and so on for the m th iteration,

$$\frac{\partial \phi_{\text{inn}}^{(m)}}{\partial \nu_{\text{inn}}} + ik\phi_{\text{inn}}^{(m)} = 2ik \sum_{j=0}^{m-1} (\phi_{\text{out}}^{(j)} - \phi_{\text{inn}}^{(j)}), \quad (40)$$

$$\frac{\partial \phi_{\text{out}}^{(m)}}{\partial \nu_{\text{out}}} + ik\phi_{\text{out}}^{(m)} = 2ik\phi_{\text{inn}}^{(m)} - 2ik \sum_{j=0}^{m-1} (\phi_{\text{out}}^{(j)} - \phi_{\text{inn}}^{(j)}). \quad (41)$$

APPENDIX B: DERIVATION OF THE BOUNDARY ERROR ENERGY EQUATION

In [1] Després proved that if e is the weak solution for the Helmholtz equation in the domain Ω , then on the boundary $\partial\Omega$ we have

$$\int_{\partial\Omega} |(\partial_\nu + ik)e|^2 = \int_{\partial\Omega} |(\partial_\nu - ik)e|^2 = \int_{\partial\Omega} |\partial_\nu e|^2 + k^2|e|^2. \quad (42)$$

Using this result, the energy defined by Eq. (27) can be written for one subdomain Ω_i as

$$\begin{aligned} E_i^{m+1} &= \int_{\partial\Omega_i} |(\partial_{\nu_i} + ik)e_i^{m+1}|^2 - (\alpha - k)^2 \int_{\Gamma_i} |e_i^{m+1}|^2 \\ &= \int_{\Sigma_{ij}} |(\partial_{\nu_i} + ik)e_i^{m+1}|^2 + \int_{B_i} |(\partial_{\nu_i} + ik)e_i^{m+1}|^2. \end{aligned}$$

The last two integrals can be written in terms of the solution at the previous iteration according to Eqs. (25) and (26),

$$E_i^{m+1} = \sum_k \int_{\Sigma_{ik}} |(-\partial_{\nu_k} + ik)e_k^m|^2 + \int_{B_i} |(\mathcal{M}e^m)_i + ik e_i^m|^2,$$

where the sum is performed for all subdomains Ω_k adjacent to Ω_i .

The energy for all subdomains will be

$$\begin{aligned} E^{m+1} &= \sum_i E_i^{m+1} \\ &= \sum_j \int_{\partial\Omega_j} |(-\partial_{\nu_j} + ik)e_j^m|^2 - (\alpha - k)^2 \sum_j \int_{\Gamma_j} |e_j^m|^2 \\ &\quad - \sum_j \int_{B_j} |(-\partial_{\nu_j} + ik)e_j^m|^2 + \int_B |(\mathcal{M}e^m) + ik e^m|^2 \\ &= E^m + \int_B (|\mathcal{M}e^m + ik e^m|^2 - |-\partial_\nu e^m + ik e^m|^2). \end{aligned}$$

The second part of Eq. (28) is obtained by using the identity true for any two complex numbers z_1 and z_2 ,

$$|z_1 + iz_2|^2 = |z_1|^2 + |z_2|^2 + 2\Im(\bar{z}_2 z_1),$$

where \bar{z}_2 is the complex conjugate of z_2 and \Im denotes the imaginary part.

ACKNOWLEDGMENTS

This work was supported by the National Science Foundation under Grant NSF-ECS-9527169.

REFERENCES

1. B. Després, Décomposition de domaine et problème de Helmholtz, *C.R. Acad. Sci. Paris* **311**, 313 (1990).
2. H. M. Atassi, Unsteady aerodynamics of vortical flows: Early and recent developments, in *Aerodynamics and Aeroacoustics*, edited by K. Y. Fung (World Scientific, Singapore, 1994), p. 121.
3. A. S. Lyrintzis, Review: The use of Kirchhoff's method in computational aeroacoustics, *J. Fluids Eng.* **116**, 665 (1994).
4. H. M. Atassi, M. P. Dusey, and C. M. Davis, Acoustic radiation from a thin airfoil in nonuniform subsonic flows, *AIAA J.* **31**, 12 (1993).
5. J. R. Scott and H. M. Atassi, A finite-difference, frequency-domain numerical scheme for the solution of the gust response problem, *J. Comput. Phys.* **119**, 75 (1995).
6. C. M. Davis and H. M. Atassi, The far field acoustic pressure of an airfoil in nonuniform subsonic flows, in *ASME Symposium on Flow Noise Modeling, Measurement, and Control, NCA, 1991*, Vol. 11, p. 107.
7. S. M. Patrick, C. M. Davis, and H. M. Atassi, Acoustic radiation from a lifting airfoil in nonuniform subsonic flows, in *Computational Aero- and Hydro-acoustics, ASME-FED, 1993*, Vol. 147, edited by R. R. Mankbadi, A. S. Lyrintzis, O. Baysal, L. A. Povinelli, and M. Y. Hussaini, p. 41.
8. H. Lamb, *Hydrodynamics*, 3rd ed. (Cambridge Univ. Press, Cambridge, 1906).
9. J. B. Keller and D. Givoli, Exact Non-reflecting boundary conditions, *J. Comput. Phys.* **82**, 172 (1989).
10. I. Harari and T. J. R. Hughes, Analysis of continuous formulations underlying the computation of time-harmonic acoustics in exterior domains, *Comput. Methods Appl. Mech. Eng.* **97**, 103 (1992).
11. M. J. Grote and J. B. Keller, On nonreflecting boundary conditions, *J. Comput. Phys.* **122**, 231 (1995).
12. O. G. Ernst, A finite-element capacitance matrix method for exterior Helmholtz problems, *Numer. Math.* **75**, 175 (1996).
13. D. Givoli, *Numerical Methods for Problems in Infinite Domains*, Studies in Applied Mechanics, Vol. 33 (Elsevier, Amsterdam, 1992).
14. M. Malhotra and P. M. Pinsky, A matrix-free interpretation of the nonlocal Dirichlet-to-Neumann radiation boundary condition, *Int. J. Num. Meth. Eng.* **39**, 3705 (1996).
15. J. D. Benamou and B. Després, A domain decomposition method for the Helmholtz equation and related optimal control problems, *J. Comput. Phys.* **136**, 68 (1997).
16. X.-C. Cai, M. Casarin, F. Elliott, and O. B. Widlund, Overlapping Schwarz algorithms for solving Helmholtz's equation, in *Proc. 10th Int. Conf. on Domain Decomposition Methods, Providence, 1998*, edited by X.-C. Cai, C. Fahrat, and J. Mandel.